RFA Lowers IDO Activity and Slows Non-Ablated Lesion Growth in Multifocal Hepatic Carcinoma

Kailin Wang
The First Affiliated Hospital of Guangdong Pharmaceutical University
Jun Mao
Sun Yat-sen University
Siyue Mao
Sun Yat-sen University Cancer Center
Xicheng Wang
The First Affiliated Hospital of Guangdong Pharmaceutical University
Wanlin Tan
Sun Yat-sen University Cancer Center
Jun Dong (dongjun1@sysucc.org.cn)
Sun Yat-sen University Cancer Center https://orcid.org/0000-0002-1352-2567

Research Article

Keywords: Radiofrequency ablation, Indoleamine 2,3-dioxygenase, enzyme-linked immunosorbent assay, high-performance liquid chromatography, alpha-fetoprotein

Posted Date: June 29th, 2021

DOI: https://doi.org/10.21203/rs.3.rs-653609/v1

Abstract

Background: The aim of this study was to determine whether radiofrequency ablation (RFA) could activate immunity and slow non-ablated lesion growth in multifocal hepatic carcinoma.

Methods: We performed a retrospective study on patients with multifocal hepatic carcinoma and assessed the non-ablated lesion growth rate between patients who received RFA and those who did not. In self-controlled study, before and three weeks after RFA, blood samples were collected from patients who received RFA to allow for comparisons of the alpha-fetoprotein (AFP) level, indoleamine 2,3-dioxygenase (IDO) concentration as assessed by enzyme-linked immunosorbent assay (ELISA) and IDO activity as assessed by high-performance liquid chromatography (HPLC).

Results: A total of 66 patients were included in the retrospective analysis: there were 46 (69.7%) patients in the treatment group and 20 (30.3%) patients in the control group. The mean growth rate of non-ablated tumors was 0.0291 ± 0.0965 mm/d in the treatment group and 0.0947 ± 0.0754 mm/d in the control group (P = 0.001). The mean concentrations of IDO before and after RFA were 15.57±4.06 ng/ml and 7.53±1.56 ng/ml in 45 eligible patients, and this difference was significant (P = 0.034). The mean IDO activity values were 29.7±22.03 and 25.25±1.75 before and after RFA, respectively (P = 0.031). AFP decreased significantly after RFA, but there was no significant correlation between the decrease in AFP and the decrease in IDO concentration and activity.

Conclusions: RFA may induce abscopal effects in hepatic carcinoma patients, manifested by a decrease in IDO concentration and activity and a slowed growth rate in non-ablated lesions.

Background

Liver cancer ranks sixth in morbidity and fourth in mortality among all types of cancer [1]. Because most patients miss the opportunity for surgery when diagnosed, radiofrequency ablation (RFA) has become an effective supplementary therapy for multifocal hepatic carcinoma. Under the guidance of imaging methods such as computerized tomography and ultrasound, the electrode is directly placed in the tumor lesions. By delivering radiofrequency energy, the tumor and adjacent tissues are devitalized. In addition, previous studies have discovered that RFA could influence the host immune microenvironment, such as increasing local dendritic cells (DC) infiltration and the expression of CD80 and CD86[2], enhancing tumor-associated antigen-specific T cell and natural killer cell responses, and increasing programmed cell death protein 1 (PD-1) expression in primary tumors [3, 4]. Dromi et al. demonstrated that RFA can degrade non-ablated lesions in murine tumor models [5], and the treatment is designed to have an abscopal effect. The concept first proposed by Mole in 1953 is that irradiation can induce non-irradiated or distant tumor lesions to shrink [6]. However, the incidence of abscopal effects is low, and these effects mostly occur in immunogenic tumors [7]. Presently, there are no reports about RFA inducing abscopal effects in humans.

The topic of immune checkpoint inhibitors is increasingly popular in tumor immune escape research. The IDO family is a group of enzymes, including IDO1, IDO2 and TDO. IDO1 is the rate-limiting enzyme of the kynurenine (Kyn) pathway [8-10]. IDO1 mediates intracellular immune suppression through mechanisms involving three proteins: general control nonderepressible 2 (GCN2), mammalian target of rapamycin (m-TOR) and aromatic hydrocarbon receptor (AhR). These first two mechanisms are mediated by activating L-Tryptophan (L-Trp) deficiency signals, such as GCN2/eukaryotic transcription initiation factor-2α (eIF-2α), and inhibiting the master signal of L- Trp adequacy, amino acid-sensing kinase 1 (GLK1)/m-TOR[11, 12]. Kyn produced by L- Trp through IDO1 is the third mechanism and is an endogenous ligand of AhR. The binding of Kyn and AhR results in the differentiation of immature CD4+ T cells into regulatory T cells and induces the expression of IDO1, further inhibiting the immune response of T cells [13] and decreasing the immunogenicity of DC[14]. Whether IDO activity changes could participate in the abscopal effects induced by RFA activation in multifocal hepatic carcinoma has not yet been studied. We investigated RFA-related abscopal effects and their mechanism.

Methods

1. Methods

1.1 Retrospective analysis

We retrospectively analyzed 66 patients with hepatoma seen at Sun Yat-sen University Cancer Center from June 2013 to July 2016. In the treatment group, patients received RFA once between two imaging examinations; in the control group, patients did not receive treatment between the two examinations.

1.1.1 Enrollment criteria

The enrollment criteria for the retrospective analysis were as follows:

(1) Patients had a measurable mass other than the ablated lesions.

(2) Patients had no other antitumor treatment between the two evaluations.

(3) Patient disease complied with the clinical or pathological diagnostic criteria for primary hepatoma.
(4) Patients had complete follow-up data.

(5) Patients had no history of liver transplant.

1.1.2 Exclusion criteria

The exclusion criteria were as follows:

(1) Patients had no measurable non-ablated lesions.

(2) Patient received anti-tumor treatment other than RFA between the two assessments.

(3) Patients were not reviewed in time.

(4) Patients were too weak to tolerate RFA.

(5) Patients had a history of chronic autoimmune diseases (e.g., Addison's disease, multiple sclerosis, Hashimoto's thyroiditis, and hypophysitis etc.)

(6) Patients had taken immunosuppressive drugs in the treatment period.

1.1.3 Tumor growth rate

We measured the diameter changes of the largest nonablated lesions and divided it by the days between the two reviews to obtain the growth rate of the tumors.

2. Materials of observing IDO

2.1 Main reagents and instruments

The main reagents included the following: Human IDO ELISA kit (eBioscience Inc.), Trp and Kyn (Sigma Company, USA), the analytical reagent potassium phosphate monobasic (KH_2PO_4) (China Hengtai Chemical Company Ltd.), the analytical reagent hydrochloric acid (China Longtai Chemical Company Ltd.), chromatographic methanol (Merck Company, Germany), ultrapure water (Prepared via the AFS-25EDI Pure Water Meter of the Millipore company, Germany), and the chemical reagent trichloroacetic acid (TCA, Damao Chemical Reagent Factory, China).

The following instruments were used: BT224S Electronic Balance (Sartorius, Germany); 5 μl, 10 μl, 50 μl, 100 μl, 200 μl, 500 μl, and 1,000 μl pipettes (Eppendorf Company, USA); PB-10 pH Meter (Sartorius, Germany); JY88-II Ultrasound Cleaning Instrument (Xinzhi Biotechnology Company Ltd.); 5417R Centrifuge (Eppendorf Company, USA); Multiskan Spectrum Enzyme Marker (Thermo Fisher, Finland); FYL-YS-100L 37 °C thermostat (China Fuyi Company); High-Performance Liquid Chromatography (HPLC) System (Waters Company, USA): Waters 2996 Ultraviolet Detector, Waters 717 Plus Automatic Sampler; and Binary HPLC with Waters 1525 Pump, Waters 474 Fluorescence Detector, and Breeze Chromatographic Workstation.

2.2 Preparation of main solutions

2.2.1 Mobile phase of HPLC

An electronic balance was used to weigh 0.1361 g KH_2PO_4 powder, which was mixed into 800 ml of ultrapure water on an electronic balance, and then the pH was adjusted to 4.0 with hydrochloric acid. Then, the volume was adjusted to 1L. The solution was mixed with pure methanol at a ratio of 3:1 for use in chromatography and treated with ultrasound for 15 minutes after filtration of the microporous membrane.

2.2.2 Kyn storage solutions (10 mmol/L)

Kyn powder (0.0208 g) was weighed, dissolved in ultrapure water, transferred into a 10 mL volumetric bottle with a glass rod, diluted in ultrapure water to 10 mL, and mixed to obtain the standard storage solution of Kyn with a concentration of 10 mmol/L. The stock solution was aliquoted into 1.5 mL Eppendorf tubes and stored in a refrigerator at -20 °C.

2.2.3 Trp storage solutions (10 mmol/L)

Trp powder (0.0204 g) was weighed with an electronic balance, dissolved in a small amount of ultrapure water, transferred into a 10 mL volumetric bottle with glass rod, diluted in 10 mL of ultrapure water, and mixed to obtain the standard Trp storage solution with a 10 mmol/L concentration. The stock solution was aliquoted into 1.5 mL Eppendorf tubes and stored in a refrigerator at -20 °C.

2.2.4 Trichloroacetic acid (30% (m/v))

Trichloroacetic acid (1.5 g) was weighed, mixed with 50 mL of ultrapure water, dissolved and moved into a brown bottle for storage at room temperature.

3.1 The assay of IDO

We measured the activity and concentration of IDO before and after RFA in patients who were newly diagnosed with primary hepatoma in our center and underwent CT-guided RFA from May 2014 to June 2016. All patients were fully aware of the risk of the operation and signed informed consent before treatment. This study was approved by the Ethics Committee of Sun Yat-sen University Cancer Center.

3.1.1 Enrollment criteria

The principal eligibility criteria were as follows:

(1) Confirmed diagnosis of primary hepatoma according to histopathological criteria or the criteria of the American Society of Hepatology for the diagnosis of hepatic carcinoma;

(2) Eastern Cooperative Oncology Group (ECOG) performance status ≤ 1;

(3) Hepatic function Child-Pugh Grading A or B;

(4) International normalized ratio <1;

(5) Platelets > 50,000/cm^3;

(6) No history of hepatic encephalopathy;

(7) Receipt and acknowledgement of informed consent.

The exclusion criteria were as follows:

(1)History of prior malignancy or previous treatment for hepatic carcinoma;

(2) Existence of uncontrolled life-threatening diseases;

(3) Incomplete follow-up data;

(4) Unclear diagnosis.

3.2 Quantitative determination of IDO concentration

Venous blood samples (3 ml) were collected in dry test tubes before and after RFA and centrifuged at 3,000 rpm for 10 minutes in a high-speed centrifuge within 2 hours of collection. Then, serum was transferred into an EP tube with a pipette and stored at - 80 °C.

3.2.1 Reagents

The standard concentration of 50 ng/ml was diluted to 50 ng/ml, 25 ng/ml, 12.5 ng/ml, 6.25 ng/ml, 3.12 ng/ml, and 0 ng/ml. Wash buffer (20 x) was diluted 20 times with ultrapure water.

3.2.2 Operational processes by ELISA

(1) The multi-welled plate was removed from the aluminum foil bag after 20 minutes at room temperature, and the sample size was calculated according to the number of standard and the number of blank control wells;

(2) Standard wells, sample wells and blank wells were set up, and blank wells had nothing added. Standard wells had different concentrations of the standards added in 50 μl;

(3) The sample wells had 10 μl of sample added, and then 40 μl of the sample diluent was added.

(4) The sample and standard wells, but not the blank wells, were incubated in a 37 °C incubator for 60 minutes with 100 μl of an antibody labeled with horseradish peroxidase.

(5) The liquid in the wells was discarded, the plate was dried via patting with absorbent paper, each well was filled with diluted wash buffer, the wells were oscillated for 30 seconds, the wash buffer was removed by forceful shaking, and the plates were dried via patting with absorbent paper; the process was repeated 5 times.

(6) The reaction substrates A (50 μl) and B (50 μl) were added to all the wells, aluminum foil was added to protect the reaction from light, and the reactions were incubated in a 37 °C incubator for 15 minutes.

(7) The optical density value of each well was determined at a wavelength of 450 nm within 15 minutes after adding 50 μl of the reaction termination solution to all the wells.

(8) The standard curve was drawn, and the concentration of each sample was calculated according to the regression curve equation (Fig. 1A).

3.3 Determination of IDO activity by HPLC

3.3.1 Standard solution preparation

(1) Kyn standard solution preparation

The prepared 10 mmol/L Kyn storage solution was absorbed and diluted to 10 mL with phosphate buffer saline (PBS). The standard solution of 50 μmol/L Kyn was obtained by vigorous stirring and shaking. The Kyn standard solutions of 10, 5, 2, 1, and 0.5 μmol/L were diluted from the standard sequentially.

(2) Trp standard solution preparation

The 10 mmol/L Trp storage solution was added into an Eppendorf tube with a pipette, and 495 μl of PBS buffer was then added. The Trp standard solution of 100 μmol/L was obtained by shaking and mixing. The standard solution of 100 μmol/L Trp was diluted to 100, 80, 50, 30, and 10 μmol/L sequentially.

3.3.2 Pretreatment of serum samples

The patient serum was removed from the refrigerator at -80 °C, thawed at room temperature, and placed in a 1.5 mL Eppendorf tube. Each tube was mixed with 150 μL of the trichloroacetic acid solution. The supernatant was centrifuged at 4 °C for 20 minutes at maximum speed. The supernatant was filtered by a microporous membrane. Finally, 400 mL of the filtrate was absorbed and added into an HPLC automatic sampling tube.

3.3.3 Pretreatment with standard solutions

The standard solutions of Kyn and Trp at different concentrations were removed from the refrigerator at -20 °C and thawed at room temperature, and 500 μL was added into a 1.5 mL Eppendorf tube, mixed with prepared 150 μL trichloroacetic acid, and centrifuged at 4 °C for 20 minutes at maximum speed. The supernatant was filtered with a microporous membrane, and then 400 μL of the filtrate was transferred into an HPLC automatic sampling tube.

3.3.4 Establishment of the ultraviolet detection wavelength

By measuring the maximum absorption wavelength of Kyn in the range of 300 to 400 nm, it was found that there was an expected absorption peak of Kyn at 360 nm. Therefore, 360 nm was selected as the detection wavelength for quantitative analysis of Kyn in this experiment.

3.3.5 Determination of the wavelengths for fluorescence detection

According to previous experiments, the excitation wavelength and emission wavelength of Trp were 286 nm and 360 nm, respectively.

3.3.6 Chromatographic Conditions and System Pretest

Chromatographic conditions:

Chromatographic column: Phenomenex Gemini C18 chromatographic column (250×4.60 mm, 5 μm)

Precolumn: Phenomenex Gemini C18 guard column (4×30 mm)

Column temperature: room temperature

Detection time of each sample: 10 minutes

Mobile phase: buffer solution of 1 mmol/L KH2PO4 (pH=4.0) and carbinol (75:25, v/v)

Current Speed: 1.0 mL· $minute^{-1}$

Injection sample size: 20 μL.

Ultraviolet detection wavelength: 360 nm

Fluorescence excitation wavelength: 286 nm

Fluorescence emission wavelength: 360 nm

The separation degree of Trp and Kyn was 1.2, and the number of theoretical trays was not less than 10,000. The chromatogram of the standard sample was drawn, as shown in Fig. 1B and Fig. 1C. The average retention time of the Trp standard sample was 6.430 minutes and that of the Kyn standard sample was 5.031 minutes.

3.3.7 Protraction standard curves

(1) Creation of the Kyn standard curve

The low-concentration standard solution of Kyn was detected by HPLC. The area of the ultraviolet absorption peak was taken as the ordinate, and the actual concentrations of the standard solutions (7.692, 3.846, 1.538, 0.769, and 0.385 μmol/L) were used as abscissa. The regression equation and correlation coefficient were obtained by linear regression, and the linear regression equation was obtained by Excel software (as shown in Fig. 1D). The linear regression equation was y=3,152.5x-1,005.1, with R^2=0.99921.

(2) Creation of the Trp standard curve.

The standard solution of Trp was also analyzed by HPLC. Using the fluorescence absorption peak areas as longitudinal coordinates, the actual concentrations of Trp solutions (76.92, 61.54, 38.46, 23.08, and 7.692 μmol/L) were used as abscissa. Linear regression was used to obtain regression equations and

correlation coefficients, and the resulting linear regression equation was y = 938,719x-997,092, with R^2 = 0.99929 (as shown in Fig. 1E).

3.3.8 Calculation of IDO Activity

The concentration of Kyn and Trp in the samples was determined according to the standard curve drawn by the external standard method. The calculated concentration was multiplied by the dilution (1.3) during pretreatment, and that represented the Trp concentration in the sample. The activity of IDO was expressed as the ratio of Trp concentration to Kyn concentration (Trp/Kyn). When increases in IDO activity induced enhanced Trp metabolism, the concentration of Kyn was increased, and the ratio was reduced.

4. Statistical analysis

We used a chi-square test or Fisher's exact test to compare the clinical characteristics of all patients. Using the Kolmogorov-Smirnov test and nonparametric testing of two independent samples (Mann-Whitney test), we compared the tumor growth rate. We used a paired Student’s t test to compare IDO concentration and activity before and after treatment, and the correlation analyses comparing the differences in IDO concentration and activity before and after treatment with the differences in AFP before and after treatment used the Spearman test. Each statistical test was two-sided; $P < 0.05$ was deemed to have statistical significance. SPSS version 19.0 (IBM Corp, Armonk, NY, USA) was employed in performing all statistical analyses.

Results

1.1 Baseline characteristics of the patients in this retrospective study

Of the 66 patients in the retrospective analysis, 46 (69.7%) patients received one RFA treatment (treatment group), and 20 (30.3%) patients did not receive RFA treatment (control group) between the two imaging evaluations. 39 patients in the treatment group and 17 patients in the control group had hepatitis B virus (HBV) and/or hepatitis C virus (HCV) infection. In the treatment group, 9 (19.6%) patients had surgery, and 8 (40%) patients had surgery in the control group. In the treatment group, 9 (19.6%) patients had venous tumor embolism, and 2 (4.3%) patients had ascites. The details are shown in Table 1.

Table 1
Baseline characteristics of the 66 patients in retrospective case-controlled study.

Characteristic	Treatment Group		Control Group		Total		*P*
	No.	%	No.	%	No.	%	
Age							0.117*
≤50	8	17.4	7	35.0	15	22.7	
>50	38	82.6	13	65.0	51	77.3	
Sex							0.049*
Male	43	93.5	15	75.0	58	87.9	
Female	3	6.5	5	25.0	8	12.1	
Hepatitis							0.982*
No	7	15.2	3	15.0	10	15.2	
Yes	39	84.8	17	85.0	56	84.8	
Ascites							0.483*
No	44	95.7	20	100.0	64	97	
Yes	2	4.3	0	0.0	2	3	
Tumor embolus							0.030*
No	37	80.4	20	20	57	86.4	
Yes	9	19.6	0	0.0	9	13.6	
Surgery							0.081*
No	37	80.4	12	60.0	49	74.2	
Yes	9	19.6	8	40.0	17	25.8	
*Chi-square test or Fisher's exact test							

1.2 Tumor growth rate

The mean non-ablated lesion tumor growth rate was 0.0291 ± 0.0965 mm/d in the treatment group and 0.0947 ± 0.0754 mm/d in the control group. Patients who had RFA treatment showed slower tumor growth than those who were not treated, and the difference was statistically significant ($P = 0.001$) (Fig. 2 and Fig. 3).

2.1 Baseline characteristics for patients who had IDO levels tested

In total, 45 eligible patients had their IDO levels tested. Males accounted for 88.9% of the participants, and females accounted for 11.1%. The average age of the patients was 55.6 years. Among them, 42 (93.3%) patients had hepatocellular carcinoma (HCC), and the others had cholangiocarcinoma. According to the seventh edition of the American Joint Committee on Cancer (AJCC) staging system, 7 (15.6%) patients had stage I disease, 16 (35.6%) patients had stage II disease, and 22 (48.9%) patients had stage III disease. 10 patients had jaundice, and 1 patient had ascites. Most of the patients were male, middle-aged (> 50 years), HCC, ECOG score 1–2, and HBV patients. The details are shown in Table 2.

Table 2
Baseline characteristics of the 45 patients who detected IDO activity and concentration

Charecteristics	Sample	Rate (%)
Sex		
Male	40	88.9
Female	5	11.1
Age		
≥ 50	32	71.1
< 50	13	28.9
Pathological type		
Cholangocellular carcinoma	3	6.7
Hepatocellular carcinomar	42	93.3
Stage		
I	7	15.6
II	16	35.6
III	22	48.9
ECOG		
0	4	8.9
1	31	68.9
2	10	22.2
Jaundice	10	22.2
HBV	30	66.7
Ascite	1	2.2

2.2 IDO activity and concentration

The mean IDO concentrations before and after RFA were 15.57 ± 4.06 ng/ml and 7.53 ± 1.56 ng/ml, respectively, which was a significant difference (P = 0.034). The mean IDO activity scores before and after RFA were 29.7 ± 22.03 and 25.25 ± 1.75, respectively. There was a significant difference between the two groups (P = 0.031). The details are shown in Table 3.

Table 3
Comparison of IDO results before and after treatment

Time	IDO activity	IDO concentration (ng/ml)
Before treatment	29.72 ± 2.03	15.57 ± 4.06
After treatment	25.25 ± 1.75	7.53 ± 1.56
*P***	0.034	0.031
**Student's *t*-test		

2.3 The correlation of AFP and IDO

The median AFP levels before and after treatment were 174.5 ng/ml (16.6950–4780.5 ng/ml) and 75.18 ng/ml (4.615–713.65 ng/ml), respectively, and the difference was statistically significant (P = 0.026). There was no correlation between the change in AFP before and after treatment and the change in IDO activity and concentration (activity P = 0.169, R = 0.209; concentration P = 0.504, R = 0.102).

Discussion

In this retrospective case-controlled study, the baseline characteristics of the treatment group and control group were balanced. The growth rate of non-ablated lesions in the treatment group was significantly slower than that in the control group (P = 0.001), and we verified that RFA can stimulate the abscopal effect; these results are in agreement with the results of Dromi et al. [5]. In the IDO analyses, the patients had indications for RFA, and most early-stage patients had undergone surgery, so there were no patients with stage IV disease and few patients with stage I-II disease. Most patients had infection with HBV, and the infection rate agreed with that in China [15, 16]. According to the ELISA results, HPLC test results and clinical AFP analysis, before and three weeks after RFA, the AFP value and the IDO concentration and activity were significantly different. These results suggest that RFA can affect tumor burden, destroy the IDO-related immunosuppressive microenvironment and reduce the systemic immune tolerance induced by IDO. In addition, the changes in IDO concentration and activity did not correlate with tumor burden, which demonstrates that the changes in IDO were induced by RFA.

According to previous studies, local tumor radiotherapy can stimulate the abscopal effect through several mechanisms. During the process of tumor cell death, calreticulin is transferred to the cell surface and captured by DCs, thereby presenting tumor antigens to activate cytotoxic T lymphocytes. Released high-

mobility group box 1 protein (HMGB1) acts as a pro-inflammatory mediator that stimulates monocytes to secrete the cytokines TNF, IL-1, IL-6 and IL-8 [17]. HMGB1 also binds to Toll-like receptor 4 (TLR4) on DCs. Degradation of tumor antigens captured by DCs is prevented to enhance the tumor antigen presentation process [18–20]. Released adenosine triphosphate binds to the purinergic receptors on DCs, leading to activation of the inflammatory process and release of interleukin-1β (IL-1β) [20]. After tumor cell disintegration, DNA can also promote the production of type I interferon (IFN) by activating the stimulator of interferon gene (STING) pathway in DCs[21]. RFA can also kill tumor cells and lead to the release of tumor-related cytokines, including tumor necrosis factor-α (TNF-α), IFN-γ, and IL-1β, which are significantly reduced and induce the production of tumor infiltration-related cytokines [4, 22]. Shi Liangrong et al. showed that RFA treatment can induce modest and short-lived growth inhibition and Treg and myeloid-derived suppressor cell expansion in the tumor microenvironment and upregulate the expression of PD-1 and programmed cell death 1 ligand 1(PDL-1) in distant tumors [23]. In addition, cytotoxic T lymphocyte-associated antigen-4 (CTLA-4) has also been observed to activate antitumor immunity in ablation treatment [2]. At present, there is no relevant report on the mechanism of IDO participating in the abscopal effect caused by RFA.

Because RFA can activate immunity, people began to seek immunosuppressive agents combined with RFA to treat tumors, thereby obtaining a sustained immune response, achieving the purpose of treating tumors and prolonging survival. Some clinical trials use RFA combined with PD-1/PDL-1 or CTLA-4 inhibitors. In NCT01853618, tremelimumab (a CTLA-4 inhibitor) was used in combination with ablation in patients with advanced HCC, and the results showed that the combination group had better survival than the monotherapy group [24]. In NCT03101475, RFA was combined with PDL-1 or CTLA-4 in patients with incurable liver metastases from colorectal cancer [25]. IDO1, as a key enzyme of the Kyn pathway mediating immunosuppression, is considered a potential small molecule target for cancer immunotherapy. Several IDO1-related immunosuppressant drugs have been developed, such as epacadostat, indoximod, navoximod (GDC-0919), and BMS 986205 [26]. In NCT01685266 and NCT00567931, IDO1 inhibitor monotherapy did not show any benefit in solid tumors [27, 28]. A previous in vivo study by Stefani Spranger et al. showed that the expression of IDO1 was upregulated with anti-CTLA-4 or anti-PD-1/PD-L1 treatment; as such, researchers are gradually exploring combination therapy [29]. In ECHO-202/KEYNOTE-037, patients received epacadostat combined with pembrolizumab (a PD-1 inhibitor), which showed good tolerability and safety [30]. In addition, combination therapies in the first-line setting in melanoma and in the second-line setting in non-small-cell lung cancer and head & neck cancer showed superior overall response rates compared with pembrolizumab [31]. Clinical trials of other IDO inhibitors combined with anti-angiogenesis agents, peptide vaccines, etc., are also in full swing given the interest in the potential synergistic interactions of these therapies [31]. We expect future clinical trials of IDO1 inhibitors combined with RFA treatment in liver cancer.

We used a retrospective analysis to confirm that RFA can reduce non-ablated lesions and simulate abscopal effects. ELISA and HPLC were used to dynamically track the immunosuppressive factors related to IDO in patients with hepatic carcinoma, and values before and after RFA treatment were compared. It was confirmed that RFA could effectively reduce the tumor burden, the concentration of IDO

and the activity of IDO in serum to a certain extent. Some of these findings are of great significance for reducing the immunosuppression of tumors. This study also had several limitations, including errors in the ELISA data, inadequate collection of blood samples, and the retrospective nature of this study, which looked at the tumor growth rate in untreated lesions, which will be improved in future studies.

Conclusions:

RFA can slow the growth of non-ablated lesions and activate abscopal effects. Additionally, it can reduce tumor burden and decrease the concentration and activity of IDO in peripheral blood, reducing immunosuppression.

Abbreviations

RFA: radiofrequency ablation; AFP: alpha-fetoprotein; IDO: indoleamine 2,3-dioxygenase; HPLC: high-performance liquid chromatography; ELISA: enzyme-linked immunosorbent assay; DC: dendritic cell; Kyn: kynurenine; Trp: Tryptophan ; GCN2: general control nonderepressible 2; m-TOR: mammalian target of rapamycin; AhR: aromatic hydrocarbon receptor; eIF-2α: eukaryotic transcription initiation factor-2α; ECOG: Eastern Cooperative Oncology Group; PBS: phosphate buffer saline; HBV: hepatitis B virus; HCV: hepatitis C virus; AJCC: American Joint Committee on Cancer; HMGB1: high-mobility group box 1 protein; IL-1β: interleukin-1β; STING: stimulator of interferon gene; IFN: interferon; TNF-α: tumor necrosis factor-α; PD-1: Programmed cell death protein 1; PDL-1: programmed cell death 1 ligand 1; CTLA-4: cytotoxic T lymphocyte-associated antigen-4; HCC: hepatocellular carcinoma;

Declarations

Ethics approval and consent to participate

The current study was approved by the Institutional Review Board of Sun Yat-sen University Cancer Center, and all procedures met the basic standards of the Declaration of Helsinki.

Ethics, consent, and permissions: All patients were clearly informed of the potential risks and benefits before undergoing the procedure. All patients stated their understanding and signed the informed consent form voluntarily.

Consent to participate: All patients were clearly informed of the potential risks and benefits before undergoing the procedure. All patients stated their understanding and signed the informed consent form voluntarily.

Consent for publication

All patients consented for publication voluntarily.

Availability of data and material

The dataset(s) supporting the conclusions of this article is (are) available in the public Research Data Deposit platform (www.researchdata.org.cn) with the approval RDD number RDDA2019001297.

Competing of interests

The authors declare that they have no competing interests.

Funding

This project was supported by the National Science Foundation for Young Scholars of China (Grant Nos. 81601581 and 81600606).

Authors' contributions

KW and JM contributed to drafting and editing of the manuscript, deserving the first authorship. WT and JD designed, revised and finalized the manuscript. YH and YX participated in revision and coordination, and contributed to literature search. XW participated in revision and coordination. All authors contributed to data analysis, drafting and revising the paper and agreed to be accountable for all aspects of the work. All authors read and approve the final manuscript.

Acknowledgments

We would like to express our gratitude to the research staff at the department for their outstanding work and dedication.

References

[1] F. Bray, J. Ferlay, I. Soerjomataram, R.L. Siegel, L.A. Torre, A. Jemal, Global cancer statistics 2018: GLOBOCAN estimates of incidence and mortality worldwide for 36 cancers in 185 countries, CA: a cancer journal for clinicians, 68 (2018) 394-424.

[2] M.H. den Brok, R.P. Sutmuller, S. Nierkens, E.J. Bennink, C. Frielink, L.W. Toonen, O.C. Boerman, C.G. Figdor, T.J. Ruers, G.J. Adema, Efficient loading of dendritic cells following cryo and radiofrequency ablation in combination with immune modulation induces anti-tumour immunity, British journal of cancer, 95 (2006) 896-905.

[3] A. Zerbini, M. Pilli, D. Laccabue, G. Pelosi, A. Molinari, E. Negri, S. Cerioni, F. Fagnoni, P. Soliani, C. Ferrari, G. Missale, Radiofrequency thermal ablation for hepatocellular carcinoma stimulates autologous NK-cell response, Gastroenterology, 138 (2010) 1931-1942.

[4] A. Zerbini, M. Pilli, A. Penna, G. Pelosi, C. Schianchi, A. Molinari, S. Schivazappa, C. Zibera, F.F. Fagnoni, C. Ferrari, G. Missale, Radiofrequency thermal ablation of hepatocellular carcinoma liver nodules can activate and enhance tumor-specific T-cell responses, Cancer research, 66 (2006) 1139-1146.

[5] S.A. Dromi, M.P. Walsh, S. Herby, B. Traughber, J. Xie, K.V. Sharma, K.P. Sekhar, A. Luk, D.J. Liewehr, M.R. Dreher, T.J. Fry, B.J. Wood, Radiofrequency ablation induces antigen-presenting cell infiltration and amplification of weak tumor-induced immunity, Radiology, 251 (2009) 58-66.

[6] R.H. Mole, Whole body irradiation; radiobiology or medicine?, The British journal of radiology, 26 (1953) 234-241.

[7] K. Reynders, T. Illidge, S. Siva, J.Y. Chang, D. De Ruysscher, The abscopal effect of local radiotherapy: using immunotherapy to make a rare event clinically relevant, Cancer treatment reviews, 41 (2015) 503-510.

[8] D.H. Munn, M. Zhou, J.T. Attwood, I. Bondarev, S.J. Conway, B. Marshall, C. Brown, A.L. Mellor, Prevention of allogeneic fetal rejection by Trp catabolism, Science, 281 (1998) 1191-1193.

[9] D.H. Munn, E. Shafizadeh, J.T. Attwood, I. Bondarev, A. Pashine, A.L. Mellor, Inhibition of T cell proliferation by macrophage Trp catabolism, The Journal of experimental medicine, 189 (1999) 1363-1372.

[10] I. Theate, N. van Baren, L. Pilotte, P. Moulin, P. Larrieu, J.C. Renauld, C. Herve, I. Gutierrez-Roelens, E. Marbaix, C. Sempoux, B.J. Van den Eynde, Extensive profiling of the expression of the indoleamine 2,3-dioxygenase 1 protein in normal and tumoral human tissues, Cancer immunology research, 3 (2015) 161-172.

[11] D.H. Munn, M.D. Sharma, B. Baban, H.P. Harding, Y. Zhang, D. Ron, A.L. Mellor, GCN2 kinase in T cells mediates proliferative arrest and anergy induction in response to indoleamine 2,3-dioxygenase, Immunity, 22 (2005) 633-642.

[12] R. Metz, S. Rust, J.B. Duhadaway, M.R. Mautino, D.H. Munn, N.N. Vahanian, C.J. Link, G.C. Prendergast, IDO inhibits a Trp sufficiency signal that stimulates mTOR: A novel IDO effector pathway targeted by D-1-methyl-Trp, Oncoimmunology, 1 (2012) 1460-1468.

[13] D.H. Munn, A.L. Mellor, Indoleamine 2,3 dioxygenase and metabolic control of immune responses, Trends in immunology, 34 (2013) 137-143.

[14] A. Kandanearatchi, B.J. Brew, The kynurenine pathway and quinolinic acid: pivotal roles in HIV associated neurocognitive disorders, The FEBS journal, 279 (2012) 1366-1374.

[15] R. Zheng, C. Qu, S. Zhang, H. Zeng, K. Sun, X. Gu, C. Xia, Z. Yang, H. Li, W. Wei, W. Chen, J. He, Liver cancer incidence and mortality in China: Temporal trends and projections to 2030, Chinese journal of cancer research = Chung-kuo yen cheng yen chiu, 30 (2018) 571-579.

[16] K.R. Wei, X. Yu, R.S. Zheng, X.B. Peng, S.W. Zhang, M.F. Ji, Z.H. Liang, Z.X. Ou, W.Q. Chen, Incidence and mortality of liver cancer in China, 2010, Chinese journal of cancer, 33 (2014) 388-394.

[17] M. Obeid, A. Tesniere, F. Ghiringhelli, G.M. Fimia, L. Apetoh, J.L. Perfettini, M. Castedo, G. Mignot, T. Panaretakis, N. Casares, D. Metivier, N. Larochette, P. van Endert, F. Ciccosanti, M. Piacentini, L. Zitvogel, G. Kroemer, Calreticulin exposure dictates the immunogenicity of cancer cell death, Nature medicine, 13 (2007) 54-61.

[18] H.E. Barker, J.T. Paget, A.A. Khan, K.J. Harrington, The tumour microenvironment after radiotherapy: mechanisms of resistance and recurrence, Nature reviews. Cancer, 15 (2015) 409-425.

[19] L. Apetoh, F. Ghiringhelli, A. Tesniere, A. Criollo, C. Ortiz, R. Lidereau, C. Mariette, N. Chaput, J.P. Mira, S. Delaloge, F. Andre, T. Tursz, G. Kroemer, L. Zitvogel, The interaction between HMGB1 and TLR4 dictates the outcome of anticancer chemotherapy and radiotherapy, Immunological reviews, 220 (2007) 47-59.

[20] M.Z. Dewan, C. Vanpouille-Box, N. Kawashima, S. DiNapoli, J.S. Babb, S.C. Formenti, S. Adams, S. Demaria, Synergy of topical toll-like receptor 7 agonist with radiation and low-dose cyclophosphamide in a mouse model of cutaneous breast cancer, Clinical cancer research : an official journal of the American Association for Cancer Research, 18 (2012) 6668-6678.

[21] L. Deng, H. Liang, M. Xu, X. Yang, B. Burnette, A. Arina, X.D. Li, H. Mauceri, M. Beckett, T. Darga, X. Huang, T.F. Gajewski, Z.J. Chen, Y.X. Fu, R.R. Weichselbaum, STING-Dependent Cytosolic DNA Sensing Promotes Radiation-Induced Type I Interferon-Dependent Antitumor Immunity in Immunogenic Tumors, Immunity, 41 (2014) 843-852.

[22] W.X. Lin, T. Fifis, C. Malcontenti-Wilson, M. Nikfarjam, V. Muralidharan, L. Nguyen, C. Christophi, Induction of Th1Immune responses following laser ablation in a murine model of colorectal liver metastases, Journal of translational medicine, 9 (2011) 83.

[23] L. Shi, L. Chen, C. Wu, Y. Zhu, B. Xu, X. Zheng, M. Sun, W. Wen, X. Dai, M. Yang, Q. Lv, B. Lu, J. Jiang, PD-1 Blockade Boosts Radiofrequency Ablation-Elicited Adaptive Immune Responses against Tumor, Clinical cancer research : an official journal of the American Association for Cancer Research, 22 (2016) 1173-1184.

[24] A.G. Duffy, S.V. Ulahannan, O. Makorova-Rusher, O. Rahma, H. Wedemeyer, D. Pratt, J.L. Davis, M.S. Hughes, T. Heller, M. ElGindi, A. Uppala, F. Korangy, D.E. Kleiner, W.D. Figg, D. Venzon, S.M. Steinberg, A.M. Venkatesan, V. Krishnasamy, N. Abi-Jaoudeh, E. Levy, B.J. Wood, T.F. Greten, Tremelimumab in combination with ablation in patients with advanced hepatocellular carcinoma, Journal of hepatology, 66 (2017) 545-551.

[25] ClinicalTrials.gov, Synergism of Immunomodulation and Tumor Ablation (ILOC).

[26] S. Yentz, D. Smith, Indoleamine 2,3-Dioxygenase (IDO) Inhibition as a Strategy to Augment Cancer Immunotherapy, BioDrugs : clinical immunotherapeutics, biopharmaceuticals and gene therapy, 32 (2018) 311-317.

[27] R. Kristeleit, I. Davidenko, V. Shirinkin, F. El-Khouly, I. Bondarenko, M.J. Goodheart, V. Gorbunova, C.A. Penning, J.G. Shi, X. Liu, R.C. Newton, Y. Zhao, J. Maleski, L. Leopold, R.J. Schilder, A randomised, open-label, phase 2 study of the IDO1 inhibitor epacadostat (INCB024360) versus tamoxifen as therapy for biochemically recurrent (CA-125 relapse)-only epithelial ovarian cancer, primary peritoneal carcinoma, or fallopian tube cancer, Gynecologic oncology, 146 (2017) 484-490.

[28] H.H. Soliman, S.E. Minton, H.S. Han, R. Ismail-Khan, A. Neuger, F. Khambati, D. Noyes, R. Lush, A.A. Chiappori, J.D. Roberts, C. Link, N.N. Vahanian, M. Mautino, H. Streicher, D.M. Sullivan, S.J. Antonia, A phase I study of indoximod in patients with advanced malignancies, Oncotarget, 7 (2016) 22928-22938.

[29] S. Spranger, H.K. Koblish, B. Horton, P.A. Scherle, R. Newton, T.F. Gajewski, Mechanism of tumor rejection with doublets of CTLA-4, PD-1/PD-L1, or IDO blockade involves restored IL-2 production and proliferation of CD8(+) T cells directly within the tumor microenvironment, Journal for immunotherapy of cancer, 2 (2014) 3.

[30] T.C. Mitchell, O. Hamid, D.C. Smith, T.M. Bauer, J.S. Wasser, A.J. Olszanski, J.J. Luke, A.S. Balmanoukian, E.V. Schmidt, Y. Zhao, X. Gong, J. Maleski, L. Leopold, T.F. Gajewski, Epacadostat Plus Pembrolizumab in Patients With Advanced Solid Tumors: Phase I Results From a Multicenter, Open-Label Phase I/II Trial (ECHO-202/KEYNOTE-037), Journal of clinical oncology : official journal of the American Society of Clinical Oncology, (2018) JCO2018789602.

[31] T. Komiya, C.H. Huang, Updates in the Clinical Development of Epacadostat and Other Indoleamine 2,3-Dioxygenase 1 Inhibitors (IDO1) for Human Cancers, Frontiers in oncology, 8 (2018) 423.

Figures

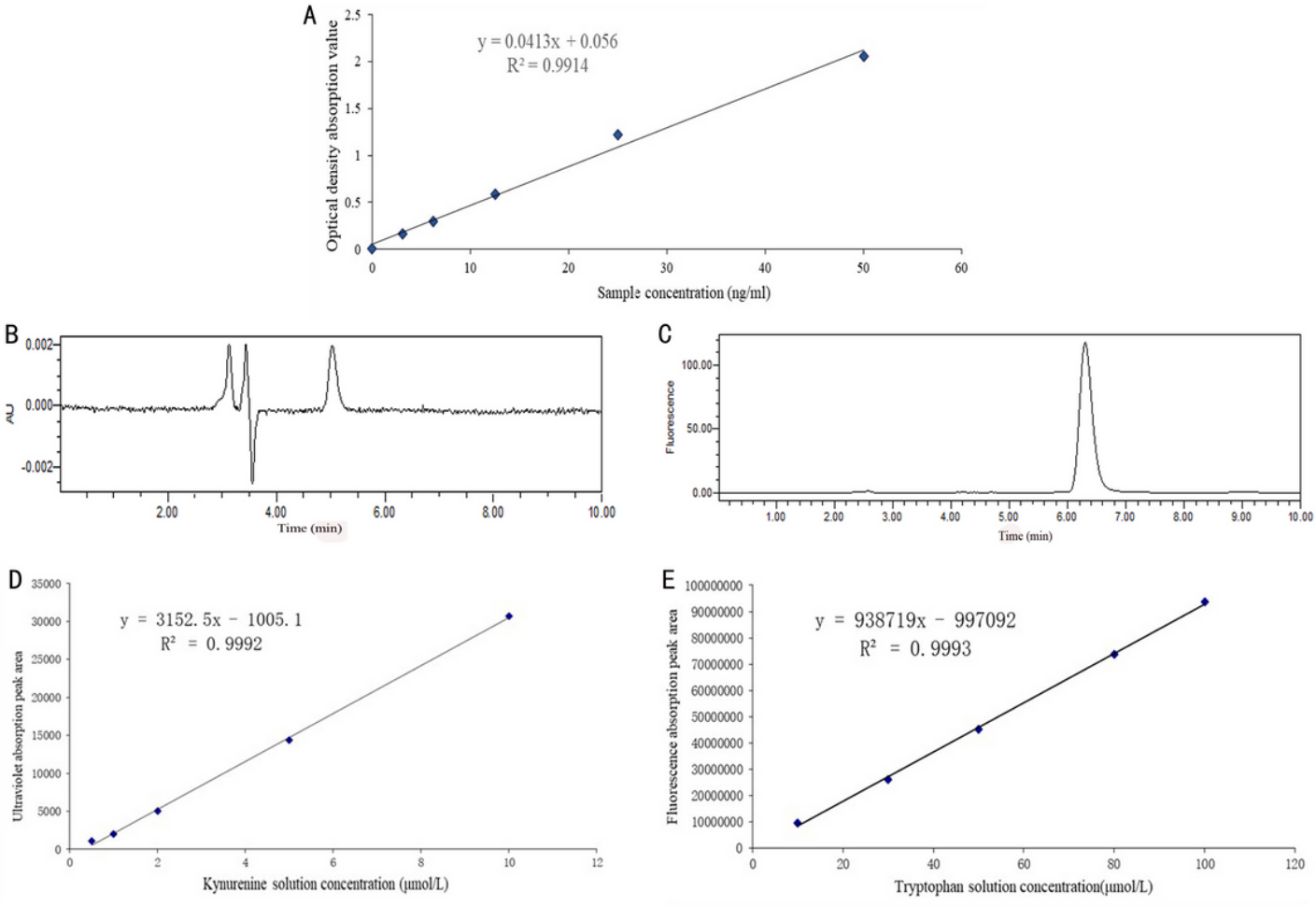

Figure 1

Standard curve of IDO concentration and activity (A) ELISA standard curve. (B) Chromatography image of the 10 μmol/L Kyn standard. (C) Chromatography image of the 50 μmol/L Trp standard. (D) Kyn standard curve and regression equation. (E) Trp standard curve and regression equation.

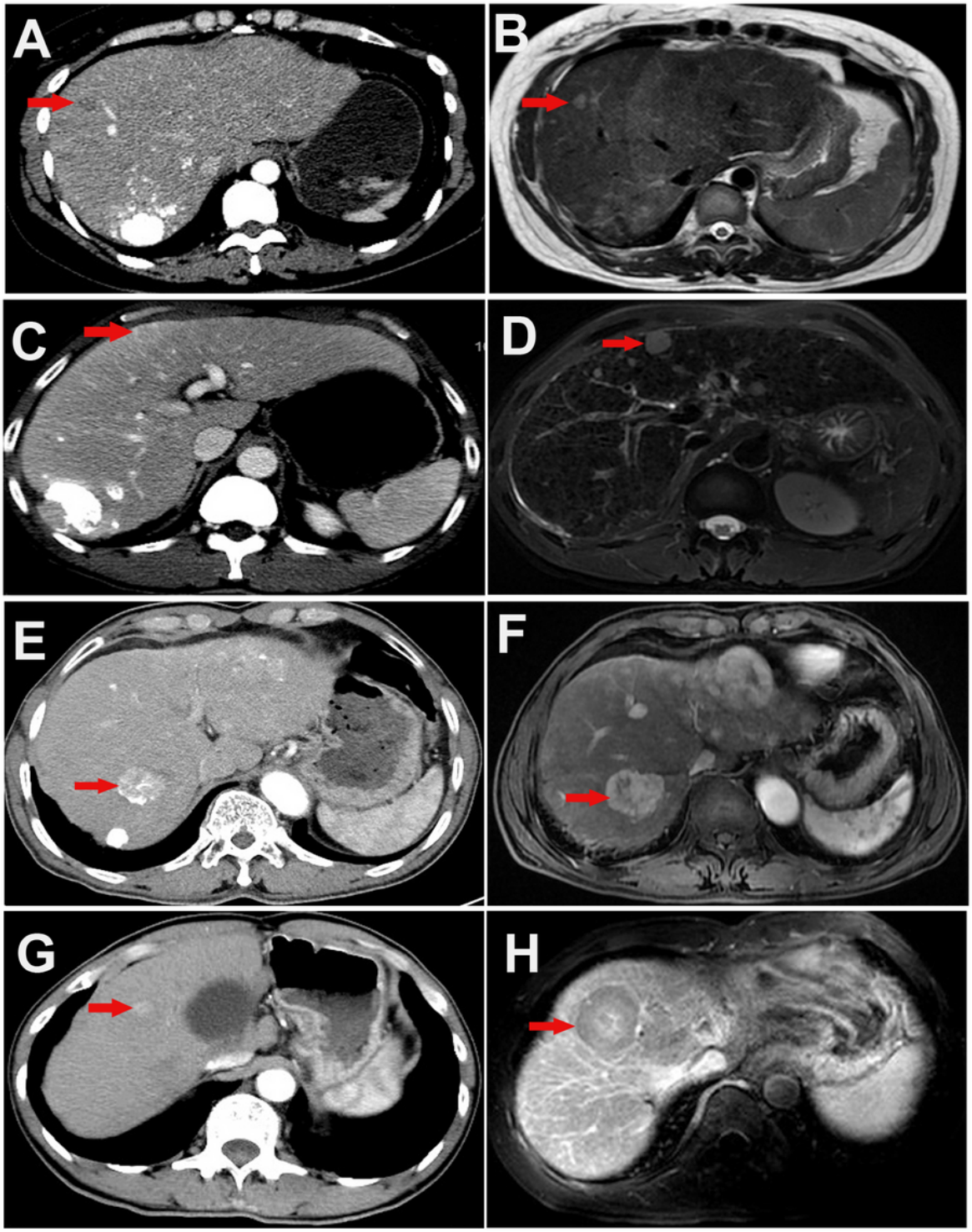

Figure 2

Images of the treatment group and control group. (A) CT imaging of a patient in the treatment group before RFA. (B) MRI of the same patient in A after RFA. (C) CT imaging of a patient in the treatment group before RFA. (D) MRI of the same patient in C after RFA. (E) CT imaging of a patient in the control group in the previous review. (F) MRI of the same patient in E in the last review. (G) CT imaging of a patient in the

control group in the previous review. (H) MRI of the same patient in G in the last review. The mass beside the RFA lesion was obviously increased in the control group compared with the treatment group.

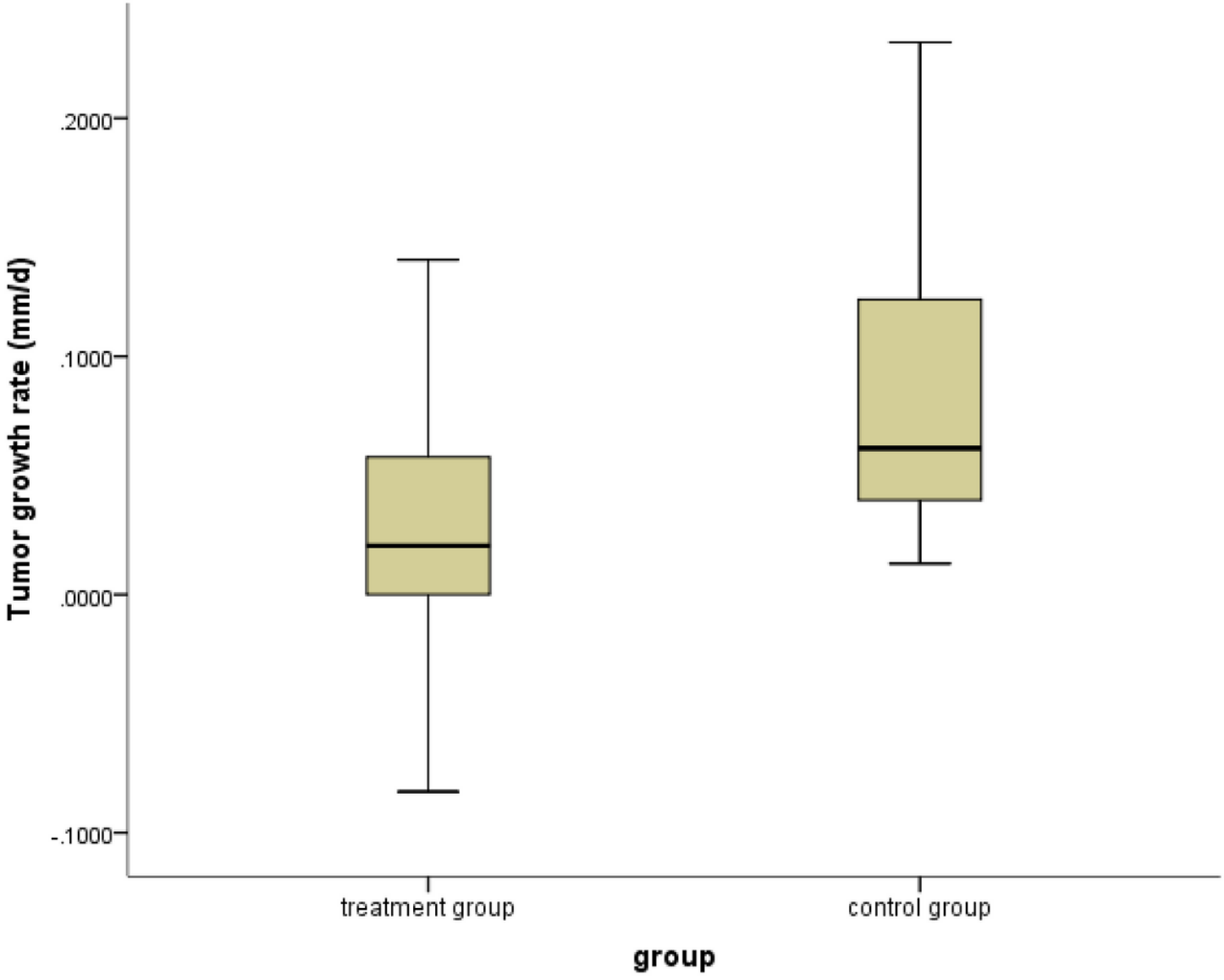

Figure 3

The tumor growth rate in the treatment group was slower than in the control group, and the difference was statistically significant (P=0.001).